JOURNAL OF Applied Polymer SCIENCE

Synthesis and Characterization of a Carboxyl-Terminated Waterborne Hyperbranched Polymer and Its Coordination Behavior with Chromium(III)

Chenying Li,[1,2] Hualin Chen,[1] Bailing Liu,[1] Bin Wang,[1,2] Rong Luo,[1] Ning Shan[1,2]

[1]Chengdu Institute of Organic Chemistry, Chinese Academy of Sciences, Chengdu 610041, China

[2]Graduate School, Chinese Academy of Sciences, Beijing 100049, China

Correspondence to: B. Liu (E-mail: blliuchem@hotmail.com)

ABSTRACT: Despite its irreplaceable position in the leather industry, chrome tanning has been listed in the procession of limitation. The serious environmental pollution caused by chrome tanning through the residual chrome it leaves in wastewater has attracted great attention. To improve the absorption of chrome and reduce chromium emission, a novel hyperbranched ligand was synthesized and characterized. The impact elements of the coordination process between the hyperbranched oligomer and Cr(III) was investigated, and the characteristics of the complex are also discussed. This hyperbranched oligomer had a low molecular weight (weight-average molecular weight = 2125) and narrow molecular weight distribution (PDI = 1.21). The time required for the coordination process between the hyperbranched oligomer and Cr(III) was around 6 h, and the optimum pH was 4.0. Moreover, the complex exhibited alkali resistance and fair resistance to oxidation; this suggested that this developed hyperbranched ligand is a potential masking agent or tanning auxiliary for chrome tanning and will enable improvements in chromium absorption. © 2013 Wiley Periodicals, Inc. J. Appl. Polym. Sci. **2014**, *131*, 40117.

KEYWORDS: adsorption; dendrimers; hyperbranched polymers and macrocycles; monomers; oligomers and telechelics; properties and characterization; structure-property relations

Received 25 March 2013; accepted 23 October 2013

DOI: 10.1002/app.40117

INTRODUCTION

An amount of 18 billion ft^2 of leather products is made globally every year, and more than 90% of them are processed through chrome-tanning technology.[1] However, 30–70% of the total Cr(III) in the leather industry is discharged from chrome-tanning process; this leads to significant chrome loss and serious pollution.[2] Therefore, minimization of the environmental impact of chrome tanning has been a hot topic for researchers.[3–6] Consequently, the promotion of chromium absorption becomes the most adoptable approach for reducing chromium contamination.

The Baychrom C series products, developed by Bayer Co., Ltd., are successful high-absorption chrome-tanning agents in the recent market. The polymer component, introduced in Baychrom C, is able to improve the chrome-absorption effectively. However, the use of the polymer component also has some drawbacks. Besides its high price, Baychrom C can only be used as a retanning agent because of its linear structure and large molecular weight. Thus, scholars have made great efforts to develop polymers with hyperbranched structures for the production of high-absorption chrome-tanning agents.[7]

The interest in hyperbranched polymers stems from their unique molecular structure and excellent performance.[8–12] Because of its ellipsoidal shape, highly branched structure, and nonentangled molecular character, the hyperbranched polymer presents a low viscosity and high solubility and reactivity; this allows for a broad range of uses. In addition, a hyperbranched polymer can be synthesized by a very straightforward procedure, such as melt polycondensation.[13–15]

In the leather industry, recent research has shown that hyperbranched polymers can be used as pretanning agents,[16] retanning agents,[17,18] tanning auxiliaries,[19,20] leather-finishing additives,[21] leveling agents, colorants, tanning sewage flocculants,[22] and so on. However, it has rarely been reported that hyperbranched polymers can be used as masking agents or tanning auxiliaries for improving chrome absorption. Their unique structure and characteristics, such as their strong coordination capability, fast speed, large ion capacity, and high selectivity,[23,24] make hyperbranched polymers a novel metal-ion-complexing agent.[25] Therefore, in this study, we aimed to synthesize waterborne hyperbranched polymers, investigate their coordination behavior, and explore their possible applications in high-absorption tanning technology.

Because the large molecular weight would make penetration difficult, we prepared a hyperbranched oligomer instead. The target products, named HBP-1*x* (where *x* indicates the reaction time in the preparation process and HBP-1*x* is the general name for this series of products), were developed through one-step self-condensation with citric acid as the basic material. The citric acid is a popular complexing agent, and AB_3 type monomers have been used to synthesize hyperbranched polymers and dendrimers for the preparation of drug-delivery systems,[26,27] gold nanoparticles,[28] and linear-dendritic thermoreversible hydrogel copolymers, among others.[29] In contrast, the one-step solution polymerization[30] used in this study was more simple and practical. We expected its successful use and high chrome absorption in this study.

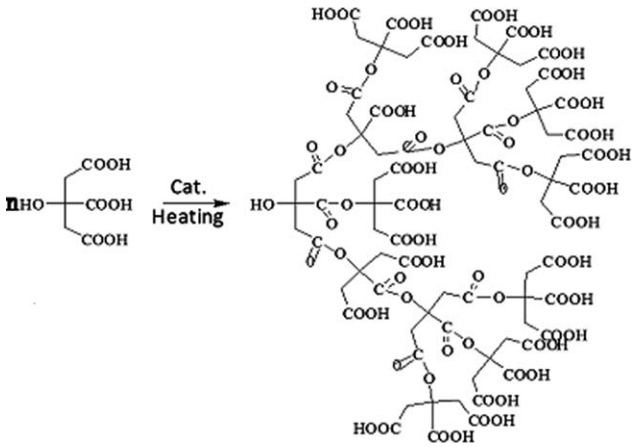

Scheme 1. Synthetic procedure for HBP-1*x*.

EXPERIMENTAL

Chemicals and Materials

Citric acid [analytical reagent (AR)], cyclohexanone (AR), *p*-toluenesulfonic acid (AR), chromium potassium sulfate dodecahydrate (AR), potassium dichromate (AR), and potassium hydroxide (AR) were purchased from Kelong Chemicals and were used as received.

Instruments and Measurements

Gel permeation chromatography (GPC) was carried out with a Waters 515 pump and a Waters 2410 refractive-index detector equipped with an OHpak KB-803 HQ column at room temperature. The polystyrene was used as the weight-average molecular weight (M_w) standard, and 0.2 mol/L $NaNO_3$ was the eluent. Differential scanning calorimetry (DSC) was carried out with a DSC Q20 V23.12 Build 103 instrument in the range from 50 to 170°C with a scanning rate of 10°C/min under a nitrogen atmosphere. NMR (AM 300-MHz NMR instrument, Bruker) was used to characterize its molecular structure with D_2O as the solvent. The Fourier transform infrared (FTIR; KBr) spectrum of the oligomer was recorded by a Nicolet MX-1E FTIR spectrometer (Nicolet, Japan).

An LVDV-C viscometer (Brookfield) was used to measure the viscosity changes in the polymerization reaction system. The acid value of HBP-1*x* was measured with a 0.10 mol/L KOH standard solution titrated in the presence of phenolphthale. The acidity of the complex solution was measured by a PHS-25 acidometer (Shweiye Instrument Factory). The electrical conductivity was measured by a DDS-11A conductivity meter (Shlei-Ci Co., Ltd). The UV absorption spectra of the complex solution was measured by a Hitachi Co. U-2010 type UV–visible spectrophotometer.

Polymerization

The HBP-1*x* was prepared as shown in Scheme 1, and the procedure was as follows. A mixture of citric acid (the monomer) and *p*-toluenesulfonic acid (the catalyst) with mass ratio of 1:0.005 was introduced into a 250-mL, four-necked flask with cyclohexanone as the solvent. The flask was set in a thermostatic oil bath equipped with mechanical stirrer, a thermometer, and a water–oil separator fitted with a condenser to collect the water from the esterification reaction. The reactant mixture was heated and kept at 125°C for given time. We monitored the esterification by measuring the viscosity of the system and the amount of collected water. By varying the reaction times at 4, 8, and 12 h, we obtained the products of HBP-1*x* with different reaction degrees and coded them as HBP-14, HBP-18, and HBP-112, respectively. Once the reaction reached the preset time, the system solvent was removed by rotary evaporation, and the product was washed with diethyl ether three times. The final product was vacuum-dried for 8 h at 60°C. Finally, the pale yellow powder was obtained. The solvent was recycled.

Factors Influencing the Coordination Reaction Between HBP-1*x* and Cr(III)

We investigated the influence of the pH, temperature, and mass ratio of Cr(III)/HBP-1*x* on the coordination reaction by measuring the changes in the pH value and the UV spectrum of the Cr(III)-HBP-112 complex solution.[31,32] HBP-112 was taken as the representative of HBP-1*x* in this study. Cr(III) solution with added HBP-112 as the ligand was the experimental group, whereas the group without HBP-112 added was the control group and was abbreviated as Cr.

Influence of pH. Three sets of 50 mL of 0.05 mol/L $KCr(SO_4)_2{\cdot}12H_2O$ aqueous solution were introduced into 100-mL beakers at 25°C, and the pH values were adjusted with $NaHCO_3$ to 3.0, 4.0, and 5.0, respectively. HBP-112 powder (1.25 g) was added to each set [the mass ratio of $KCr(SO_4)_2{\cdot}12H_2O$:HBP-112 was 1:1]. After the powder was stirred to dissolve, the pH of each set was measured and recorded as pH_0. The pH value was retested at intervals of 30 min and ΔpH ($pH - pH_0$) was calculated. The UV absorption spectra of all of the groups were measured 24 h later.

Influence of the Mass Ratio of $KCr(SO_4)_2{\cdot}12H_2O$ to HBP-112. The $KCr(SO_4)_2{\cdot}12H_2O$:HBP-112 mass ratio with 3:2, 1:1, and 2:3 were marked as Cr:H = 3:2, Cr:H = 1:1, and Cr:H = 2:3, respectively. The starting pH (pH_0) was adjusted to 4.0, and the remaining operation was the same as described in the preceding section. The changes in ΔpH in three reaction systems were recorded, and their UV adsorptions were measured 24 h later.

Influence of the Temperature. The experimental temperatures (*T*s) were 25, 35, and 45°C. A mass ratio of $KCr(SO_4)_2{\cdot}12H_2O$:HBP-112 was 3:2, and the pH_0 was adjusted to 4.0. The

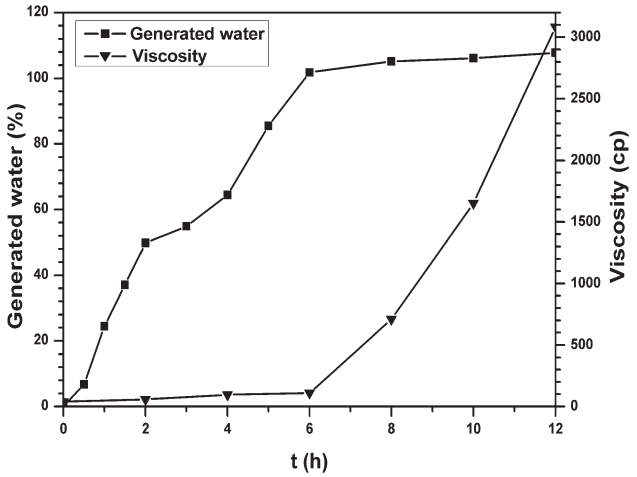

Figure 1. Changes in the water yield and viscosity with the polymerization time (t) for HBP-1x.

changes in ΔpH in three reaction systems were recorded and the UV adsorptions were measured 24 h later.

Stability of Cr(III) and HBP-1x Complex Solution

Stability of the Complex Solution Against Alkali. The samples of HBP-14, HBP-18, and HBP-112 were added to 50 mL of a 0.05 mol/L of $KCr(SO_4)_2{\cdot}12H_2O$ aqueous solution [the mass ratio of $KCr(SO_4)_2{\cdot}12H_2O$ to HBP-1x was 1:1] with stirring until the sample was dissolved. Then, the pH values of all of the solutions were regulated to 3.0 with $NaHCO_3$. These groups were denoted as Cr–HBP-114, Cr–HBP-118, and Cr–HBP-112, respectively. The control group without ligand was marked as Cr.

All of the prepared complex solutions were transferred into four 250-mL beakers; this was followed by a titration of 0.1 mol/L KOH solution. The changes in the pH and electrical conductivity in all of groups were tracked with an acidometer and conductivity meter.

Antioxidative Capacity of the Complex Solution. The same complex solutions mentioned previously were prepared, and 5 mL of 3% (w/w) H_2O_2 was added to each of the complex solutions. The solutions were magnetically stirred for 4 h. The concentration of Cr(VI) was determined through a dual-wavelength spectrophotometer.

RESULTS AND DISCUSSION

Structure of HBP-1x

HBP-1x was formed by a self-condensation esterification reaction. For the esterification process, the yield of water reflected the extent of the reaction (p), and the change in viscosity was correlated with the degree of polymerization (X_n). In Figure 1, the percentage of generated water represented the mass ratio of collected water to theoretical water yield. During the first 6 h, the amount of generated water rose rapidly from 0 to 83.5%, and then, the increase became slow. Eight hours later, the percentage of generated water reached a plateau at 106.1%. The excessive water generation shown in Figure 1 was due to some possible secondary reactions, such as decarboxylation cyclization and decomposition of citric acid under a high temperature. The viscosity of the reaction system rose slowly from 57 to 94.8 cp during the first 6 h. After that, the viscosity rose sharply. Because the esterification was a reversible reaction, the continuous removal of small molecular byproducts was required to form more ester linkages. In this experiment, cyclohexanone played a vital role as a water-carrying agent and a solvent at the same time.

According to the basic theory of condensation polymerization, in the early stage of polymerization, p already is a large value, but X_n presents very slow growth. After $p \geq 0.9$, the continuous growth of polymerization became difficult. At that time, p increased slowly, but DP grew dramatically.[33] At that point, the experimental phenomena fit the theory completely.

The acid values of the citric acid (monomer), HBP-14, HBP-18, and HBP-112 were 799.9, 773.9, 685.9, and 664.1 mg of KOH/g, respectively. As for the monomer, the relative deviation between the measured acid value (799.9 mg of KOH/g) and the theoretical acid value (801.0 mg of KOH/g) was 0.1%; this verified the accuracy of the titration operation. The acid value of the product decreased with increasing reaction time. It matched the changes in generated water and the viscosity of the reaction system.

The molecular weight and polydispersity index of the HBP-112 are presented in Figure 2. They showed that this synthetic strategy could be used to obtain a hyperbranched oligomer with a low molecular weight and low polydispersity. According to theory, the polydispersity index is around 2 when a conventional solution polymerization method is used to get the linear polyester.[33] The low polydispersity obtained here suggested that HBP-1x was different from linear polymers in molecular structure. It should be noted that the ellipsoidal, highly branched molecular structure made the molecular weight measured by GPC lower than the actual value.[34]

On the basis of the M_w obtained from GPC analysis (Figure 2), the X_n of HBP-112 was approximately 11. Thus, HBP-112

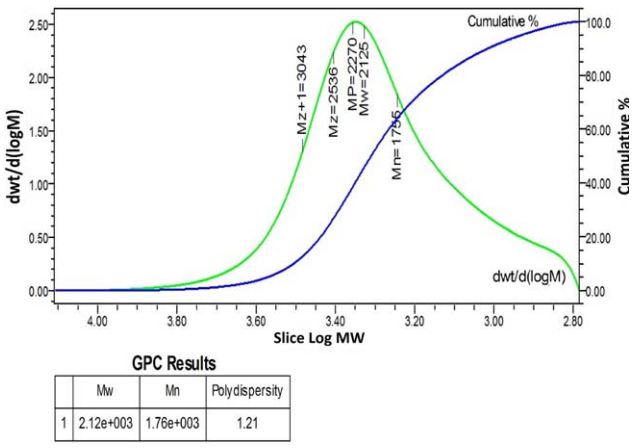

	Mw	Mn	Polydispersity
1	2.12e+003	1.76e+003	1.21

Figure 2. Molecular weights and polydispersities of HBP-112 as measured with GPC. M_n: number average molecular weight. M_w: weight average molecular weight. M_z: z-average molecular weight. M_p: molecular weight at peak value. [Color figure can be viewed in the online issue, which is available at wileyonlinelibrary.com.]

contained 23 carboxyl groups per molecule. According to the M_w and acid value of HBP-112, the number of carboxyl groups in each HBP-112 molecule was 25. These two results were similar. On the basis of eq. (1)[35] the conversion rate of hydroxyl (P_A) was about 0.909. According to Hölter et al.,[36] the degree of branching (DB) of the hyperbranched oligomer synthesized by random self-condensation with an AB_x-type monomer (AB_x = the monomer has one A functional group and $x(x>=2)$ B functional groups) can be calculated from eq. (2). In this case, citric acid was the AB_3-type monomer, which means $x = 3$. Because P_A was 0.909, the result of DB was 0.409. This result agreed well with the findings from Frey and coworkers,[37,38] in that DB was close to 0.5 when the hyperbranched polymer was synthesized by only an AB_x-type monomer:

$$\overline{X_n} = \frac{1}{1-P_A} \quad (1)$$

$$\mathrm{DB} = \frac{(1-\frac{P_A}{X})^X + P_A - 1}{\frac{(X-1)}{X} P_A} \quad (2)$$

Figure 3 shows the ^{1}H-NMR spectra of HBP-14, HBP-18, and HBP-112. The chemical shift at 4.79 was the solvent peak. The use of D_2O as the solvent made the active protons in COOH and OH exchanged, and their signal disappeared. ^{1}H-NMR spectra of HPB-1x showed a quartet at 2.80–3.04 ppm as an AB system for the CH_2 protons in HBP-1x, and the identification for the hydrogen is shown in Figure 3.[29] Because the chemical environment of CH_2 protons changed little after the esterification, the chemical shifts of CH_2 protons in HBP-1x showed no difference in the three spectra, just like the CH_2 protons of citric acid.[28,29] In Figure 4(a), the FTIR spectra indicate that C═O of ─CO─OH in the monomer had two stretching vibration absorption peaks at 1753.8 and 1712.6 cm^{-1}, respectively, because one of the ─COOH in citric acid formed an intramolecular hydrogen bond. It was this hydrogen bond that caused the C═O absorption peak to move toward a lower frequency (1712.6 cm^{-1}). The FTIR spectrum of HBP-14 was similar to that of the monomer; this implied the low level of p, and the absorption peaks of C═O (1751.9 and 1712.3 cm^{-1}) were the only one point differing from the monomer in the FTIR

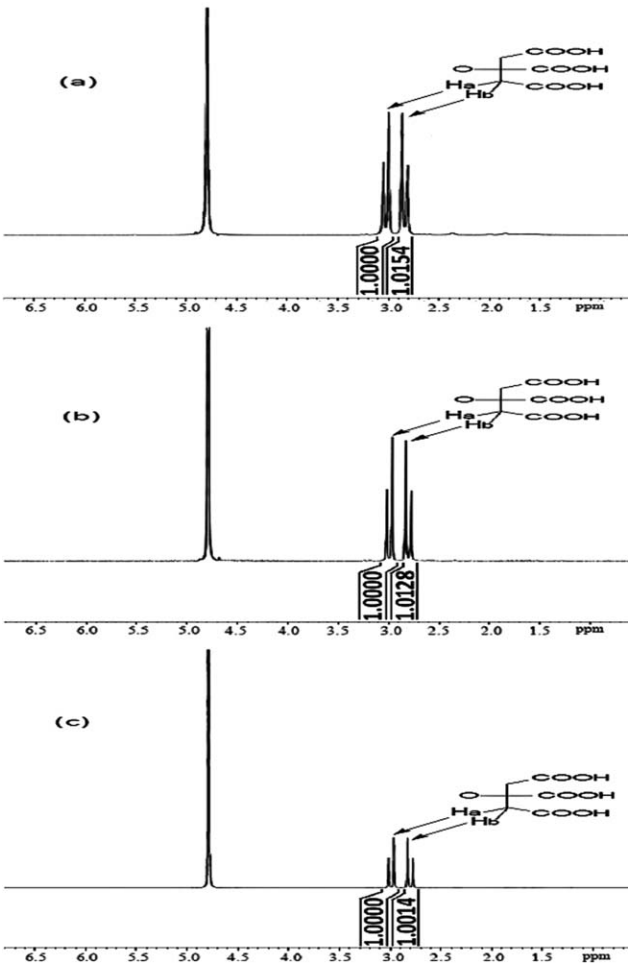

Figure 3. ^{1}HNMR spectra of (a) HBP-14, (b) HBP-18, and (c) HBP-112 in D_2O.

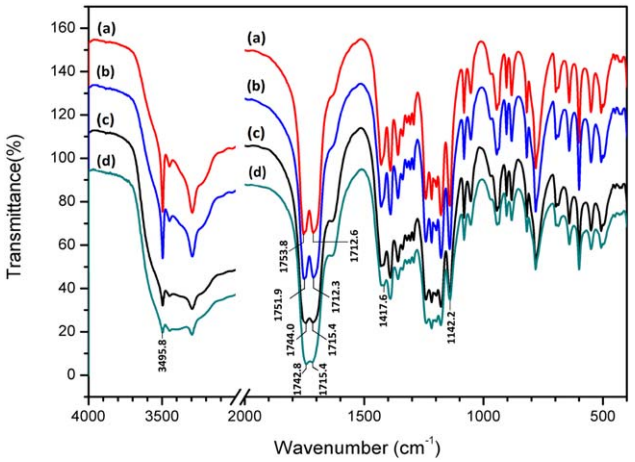

Figure 4. FTIR spectra of (a) the monomer, (b) HBP-14, (c) HBP-18, and (d) HBP-112. ($KCr(SO_4)_2.12H_2O$:HBP-112 mess ratio = 1:1, T = 25°) [Color figure can be viewed in the online issue, which is available at wileyonlinelibrary.com.]

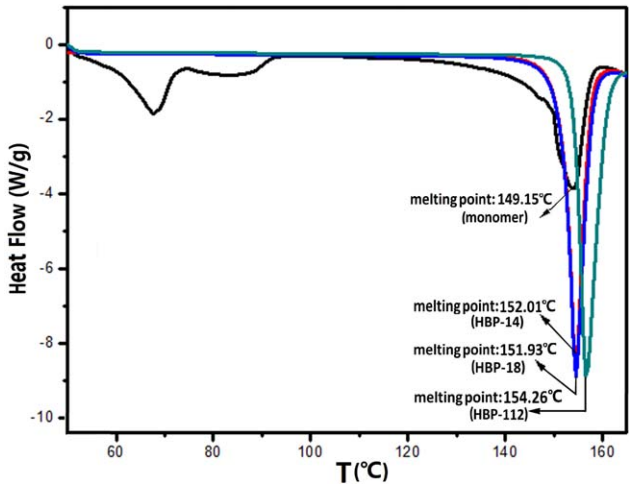

Figure 5. DSC curves of HBP-1x and the monomer. [Color figure can be viewed in the online issue, which is available at wileyonlinelibrary.com.]

Table I. Melting Points (T_m's) and Melting Enthalpies (ΔH) of HBP-1*x* and the Monomer

Item	Monomer	HBP-14	HBP-18	HBP-112
T_m (°C)	149.15	152.01	151.93	154.26
ΔH (J/g)	146.4	194.9	206.5	206.8

spectrum. However, the characteristic FTIR absorption features of HBP-18 and HBP-112 underwent some changes. For alcoholic hydroxyl groups, the bending vibration absorption of O—H (1417.6 cm^{-1}) and the vibration absorption of C—O (1142.2 cm^{-1}) become weak. The two absorption peaks of C═O in HBP-18 appeared at 1744.0 and 1715.4 cm^{-1}, and the absorption peaks of C═O in HBP-112 were found at 1742.8 and 1715.4 cm^{-1}. The changing trend of C═O absorption peaks was that the two C═O absorption peaks become closer, and the change in the left peak was greater (from 1751.9 to 1742.8 cm^{-1}) with increasing reaction time. The reason was that the carboxyl groups without the formation of hydrogen bonds were more likely to participate in the esterification reaction. Because ester groups increase with the extension of reaction time, the C═O signal of the ester groups became stronger. However, the signal of C═O in the ester groups and the signal of C═O in carboxyl were overlaying in such a case. Thus, the C═O absorption peak at 1751.9 cm^{-1} appeared to be redshifted.

As the monomer was a monohydrate crystal, its DSC curve (Figure 5) had an endothermic peak between 58 and 92°C. The large endothermic peaks at the right of the DSC curves are melting peaks. The melting enthalpy of HBP-1*x* was higher than that of the monomer and increased with the extension of the polymerization time. The melting point of HBP-1*x* was also slightly higher than that of the monomer (Table I), but the difference was trivial; this also implied a low X_n. So, we knew that the DSC test coincided with the GPC test.

Influencing Factors in the Coordination Reaction Between HBP-1*x* and Cr(III)

Cr(III) had a d^2sp^3 type of hybrid orbital and octahedral coordination structure. The coordination number was 6. Cr(III) presented the properties of hydrolytic polymerization in aqueous solution. The changes in the pH value reflected the hydrolysis of chromium and the coordination behavior with the ligand. When the terminal carboxyl groups of HBP-112 got into the complex structure through a coordinative substitution reaction, it led to a decrease in the pH value.[32] The coordination of HBP-112 and Cr(III) also made changes in the UV absorption spectra; from that, we could understand the coordination better.

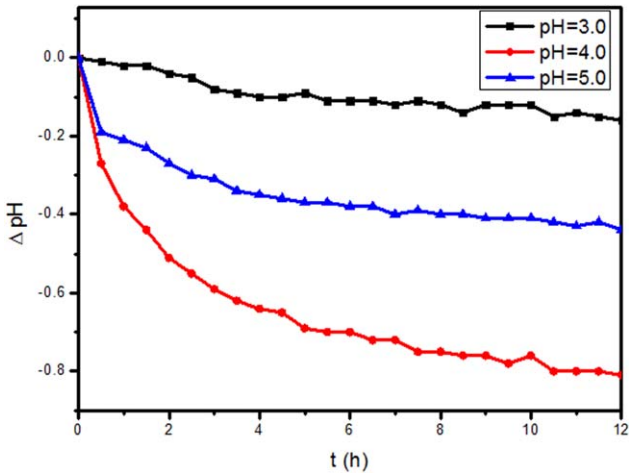

Figure 6. Changes in ΔpH with the standing time with different original pHs. ($KCr(SO_4)_2{\cdot}12H_2O$:HBP-112 mess ratio = 1:1, T = 25°C) [Color figure can be viewed in the online issue, which is available at wileyonlinelibrary.com.]

Influence of pH. Figure 6 indicates that the pH values decreased gradually in all of these systems; this indicated that there was surely a coordination reaction between HBP-112 and Cr(III) in every group, despite their different original pH. The pH decreased rapidly at the start, and then, the speed of the decrease became slower with increasing reaction time until the equilibrium was reached about 6 h later. Compared with the pH 3.0 group, when the original pH rose to 4.0, the speed of the pH decrease became faster, and the degree of pH decrease became larger. The result shows that the HBP-112 coordinated Cr(III) better when the system pH was set higher within a certain range. The pH 5.0 group, however, went against the rule. The higher pH accelerated the hydrolytic polymerization of Cr(III) and rapidly enlarged the volume of the hydrated chromium ion.[39] Too large a volume made Cr(III) difficult to coordinate with HBP-112. That was the reason why the pH 5.0 group did not show a greater pH decrease compared with the pH 4.0 group, and pH 4.0 turned out to be the optimum condition for coordination.

Under the same conditions, the characteristic absorption peaks (Table II and Figure 7) of the experimental groups with the HBP-112 ligand appeared to violetshift significantly, and the absorption intensity was increased compared with that of the control group. The increase in the initial pH enhanced the changes. With the ionization of its terminal carboxyl, the HBP-112 ligand could get into the Cr(III) complex through

Table II. Maximum Absorption Peaks and *R*s of the Complex Prepared with Different Initial pH Values

	pH = 3.0			pH = 4.0			pH = 5.0		
Complex solution	λ_{max1} (nm)	λ_{max2} (nm)	*R*	λ_{max1} (nm)	λ_{max2} (nm)	*R*	λ_{max1} (nm)	λ_{max2} (nm)	*R*
Cr-HBP-112	568	415	1.33	566	410	1.52	565	403	1.65
Cr	580	414	1.08	581	420	0.94	582	425	1.00

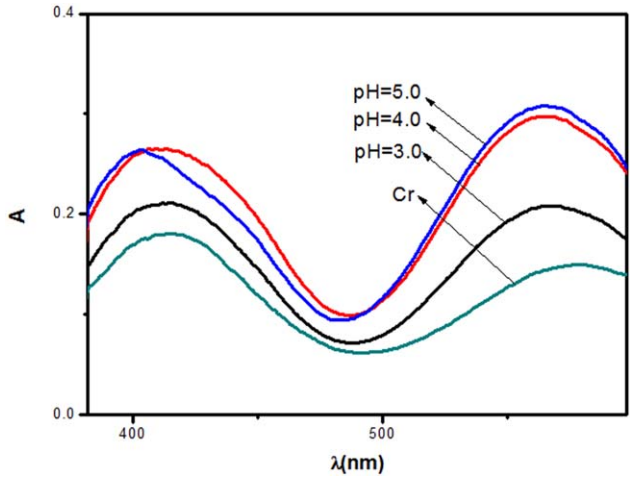

Figure 7. UV spectra of the complex prepared with different initial pH values ($KCr(SO_4)_2{\cdot}12H_2O$:HBP-112 mess ratio = 1:1, $T = 25°C$). A = Absorbance; λ = Wavelength of incident light. [Color figure can be viewed in the online issue, which is available at wileyonlinelibrary.com.]

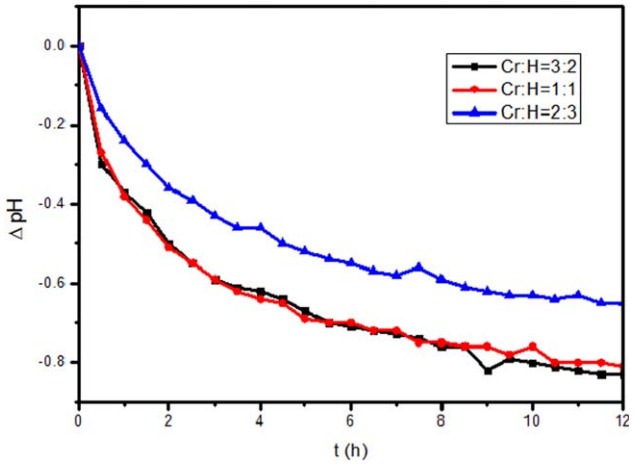

Figure 8. Changes in ΔpH with the standing time with different mess ratios of $KCr(SO_4)_2{\cdot}12H_2O$ to HBP-112 (pH = 4.0, $T = 25°C$). [Color figure can be viewed in the online issue, which is available at wileyonlinelibrary.com.]

coordination substitution and form new coordinate bonds, which changed the complex structure and led the adsorption to violetshift.

According to a literature report,[40] when the Cr(III) and ligand coordinate through chelation, the value of the molar absorption coefficient (R) in the UV adsorptions will be greater than or equal to 1.19, and the violetshift will appear (the R in Table II indicates the ratio of R values between (the wavelength of absorption peaks at around 565 nm) λ_{max1} and (the wavelength of absorption peaks at around 410 nm) λ_{max2}). Compared with control group, the addition of HBP-112 as a ligand made the R value increase significantly to a value higher than 1.19 (Table II). The experimental results matched well with the theory at this point, which indicated that HBP-1x could bind to Cr(III) through chelation. Any ligand that could bind to the central ion through chelation made the coordination compound more stable than a nonchelated coordination compound.

Influence of the Mass Ratio of Cr to HBP-112. The pH decrease in the Cr:H = 2:3 group was minimum, whereas the pH changes in other two groups were pretty similar (Figure 8) because the two curves were almost overlapping. The possible reason was that when the mass ratio of $KCr(SO_4)_2{\cdot}H_2O$:HBP-112 was 3:2, the coordination of chromium ion and the HBP-112 (oligomer ligand) reached the saturation situation. Therefore, more oligomer ligand would not bring any changes of coordination in the Cr:H = 2:3 group. In addition, the addition of more HBP-112 reduced the pH greatly; this was unfavorable for the ionization and coordination of the terminal carboxyl groups.

The high proportion of HBP-112 led to the greater violetshift in the UV adsorptions (Table III and Figure 9). With the increase in the HBP-112 proportion, more terminal carboxyl groups participated in the coordination reaction to form a new bridged bond and ring structure of complex, and this led to an increase in the violetshift.

Influence of the Temperature. Obviously, the increase in the temperature led to a faster and greater pH decrease in the complex solution. Meanwhile, the time required to reach the coordination equilibrium also gradually shortened (Figure 10). The experimental group under 25°C had a minimum pH decrease, and the pH value decreased continuously, even 8 h later. The pH in the group under 45°C had the fastest reduction rate and reached equilibrium within 3 h. The experimental group under 35°C needed 6 h to achieve the coordination equilibrium.

First of all, the hydrolysis of carboxyl groups is an endothermic reaction. The increase in the temperature intensified the hydrolysis of the terminal carboxyl, which increased the

Table III. Maximum Absorption Peaks and R Values of the Coordination Solutions with Different Mess Ratios of $KCr(SO_4)_2{\cdot}12H_2O$ to HBP-112

	Cr:H = 3:2			Cr:H = 1:1			Cr:H = 2:3		
Complex solution	λ_{max1} (nm)	λ_{max2} (nm)	R	λ_{max1} (nm)	λ_{max2} (nm)	R	λ_{max1} (nm)	λ_{max2} (nm)	R
Cr-HBP-112	568	416	1.57	566	410	1.52	567	407	1.55
Cr	—	—	—	578	414	1.07	—	—	—

pH = 4.0; $T = 25°C$.

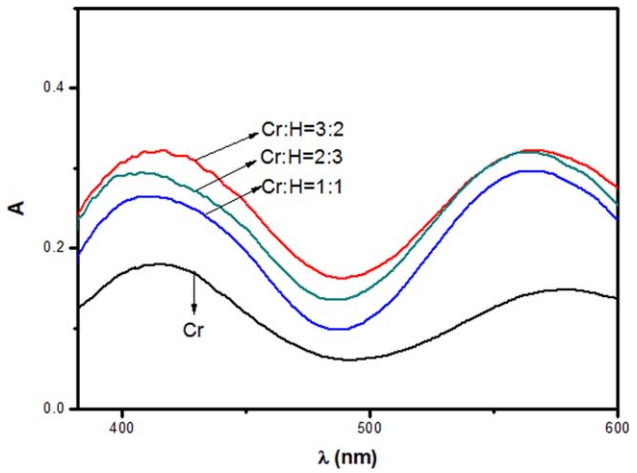

Figure 9. UV spectra of the complex prepared with different mess ratios of $KCr(SO_4)_2{\cdot}12H_2O$ to HBP-112 (pH = 4.0, T = 25°C). A = Absorbance; λ = Wavelength of incident light. [Color figure can be viewed in the online issue, which is available at wileyonlinelibrary.com.]

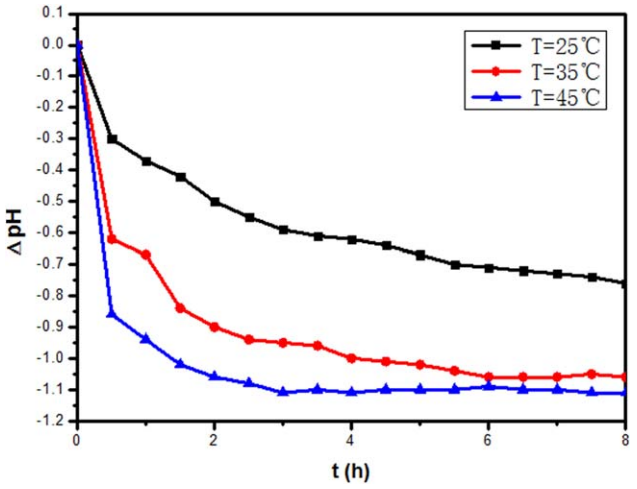

Figure 10. Changes in ΔpH with the standing time at different temperatures (pH=4.0, $KCr(SO_4)_2.12H_2O$:HBP-112 mess ratio=3:2). [Color figure can be viewed in the online issue, which is available at wileyonlinelibrary.com.]

opportunity of coordination. Second, because the hydrolysis of Cr(III) and the coordination with the carboxylate anion were both endothermic reactions, the elevated temperature was helpful for the reactions. Furthermore, the elevated temperature also promoted the reaction rate of coordination; this greatly shortened the time required to reach the coordination equilibrium. In short, the elevated temperature promoted the coordination reaction pretty well. The UV adsorptions of the complex prepared under different temperatures (Figure 11 and Table IV) matched the theory mentioned previously well.

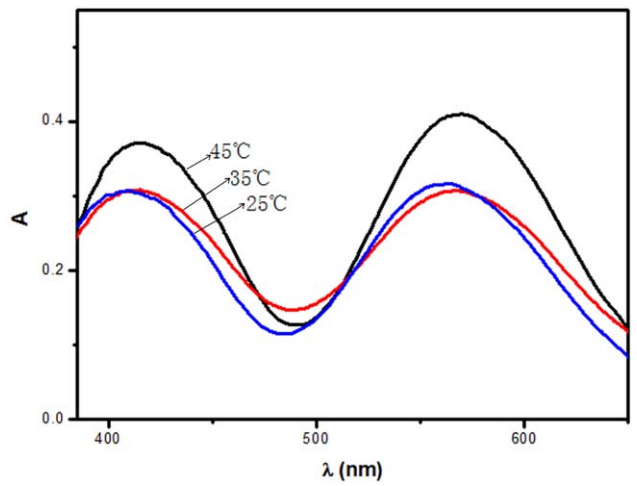

Figure 11. UV spectra of the complex prepared at different temperatures (pH = 4.0, $KCr(SO_4)_2{\cdot}12H_2O$:HBP-112 mess ratio = 3:2). A = Absorbance; λ = Wavelength of incident light. [Color figure can be viewed in the online issue, which is available at wileyonlinelibrary.com.]

Stability of the Complex Solution Formed by Cr(III) and HBP-1*x*

Stability of the Complex Solution Against Alkali. As we know, the purpose of the basifying process in chrome tanning is to promote the hydrolysis of chromium and, therefore, improve its absorption and fixation in leather. At this stage, if the alkali stability of chromium complex is poor, it will easily lead to the aggregation and precipitation of chromium; this seriously affects the penetration of chromium ions into collagen fibers and results in an overtanned leather surface and poor leather quality.[20] Therefore, the stability of the complex against alkali was surely a key point for determining whether HBP-112 could be used in development of a novel high-absorption tanning agent.

In Figure 12(a), the curve of the control group (Cr) had two plateaus. The first one represented the transformation of Cr(III) to the $Cr(OH)_3$, and most of the Cr(III) precipitated at the end of the first plateau. Because $Cr(OH)_3$ was an amphoteric

Table IV. Maximum Absorption Peaks and *R* Values of the Complex Prepared at Different Temperatures

	T = 25°C			T = 35°C			T = 45°C		
Complex solution	λ_{max1} (nm)	λ_{max2} (nm)	*R*	λ_{max1} (nm)	λ_{max2} (nm)	*R*	λ_{max1} (nm)	λ_{max2} (nm)	*R*
Cr–HBP-112	567	415	1.52	567	410	1.52	567	413	1.55
Cr	578	414	1.07	579	416	1.15	579	417	1.09

pH = 4.0; $KCr(SO_4)_2{\cdot}12H_2O$:HBP-112 mess ratio = 3:2.

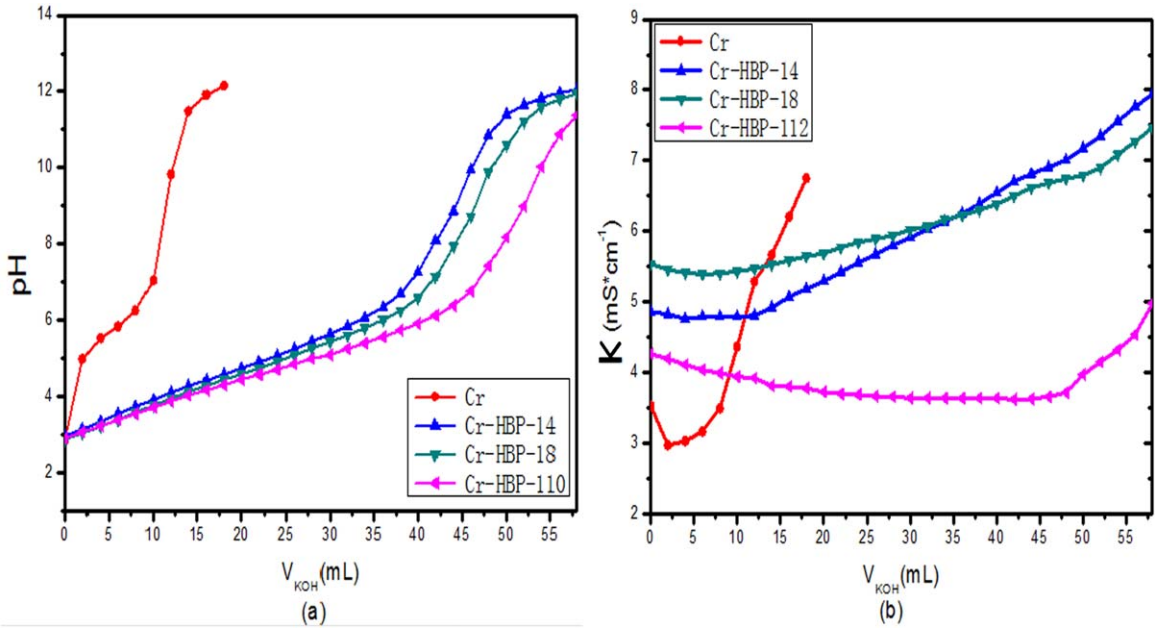

Figure 12. Addition of KOH versus the (a) pH and (b) electrical conductivity. V_{KOH} = the volume of 0.1 mol/L KOH solutions. K = electrical conductivity. [Color figure can be viewed in the online issue, which is available at wileyonlinelibrary.com.]

hydroxide, the addition of excessive alkali changed the chromium hydroxide into soluble $[Cr(OH)_4]^-$ and $[Cr(OH)_6]^{3-}$; the emergence of a second plateau in the titration curve corresponded to this change. Meanwhile, all of the experimental groups showed excellent stability against alkali. With the addition of alkali, the pH increased slowly without any precipitation, even in the alkaline environment. The pH curves of all of the experimental groups were extremely smooth compared with that of the control group. The alkali stability of the complex solutions presented the following order: Cr–HBP-14 < Cr–HBP-18 < Cr–HBP-112. With extension of the polymerization time, both polymerization degree and branched structure of the oligomer increased. This was conducive to the formation of chelation between Cr(III) and HBP-1*x*. Thus, the complex had better performance in alkali-resistance stability.

Antioxidative Capacity of the Complex Solution. There is certain amount of residual Cr(III) in chrome-tanned leather.[41] The free Cr(III) can be easily oxidized by hydroperoxides, which are generated from the oxidation of unsaturated fat liquoring agents.[42] Cr(VI) is the oxidized product of Cr(III) and is carcinogenic, and its toxicity is 100 times stronger than Cr(III). In recent years, there has been more stringent limitations on the residual Cr(VI) left in leather. In western Europe and Australia, the limitation of Cr(VI) content in leather is lower than 2 ppm.[43] Therefore, the development of novel chrome-tanning agents with an antioxidant capacity is an important target for the tanning industry. The rich terminal carboxyl groups helped HBP-1*x* to achieve good coordination with Cr(III); consequently, it radically reduced the free Cr(III), which in turn reduced the formation of Cr(VI) in leather.

The concentrations of Cr(VI) in groups denoted as Cr–HBP-114, Cr–HBP-118, and Cr–HBP-112 were 1.25×10^{-4}, 1.20×10^{-4}, and 8.80×10^{-5} mol/L, whereas the concentration of Cr(VI) in control group was 1.35×10^{-3} mol/L. Comparatively speaking, the addition of HBP-1*x*, especially HBP-18 and HBP-112, significantly reduced the formation of Cr(VI) because the polymerization degree of HBP-1*x* substantially increased after 6 h. Therefore, we concluded that the introduction of HBP-1*x* improved the antioxidant stability of the Cr(III) complex.

HBP-1*x* not only maintained citric acid's coordinating capability but also endued its coordinated complex with stability against alkali and oxidation. These will mean a great deal in its application in chrome tanning. In addition, the coordination process between the HBP-1*x* and Cr(III) was around 6 h, and the optimum pH was 4.0, which matched well with the actual requirements of the chrome-tanning process for time and pH. In addition, as the hyperbranched polymer, its low molecular weight and characteristic ellipsoidal volume will be beneficial to its penetration into collagen fibers. Therefore, the carried Cr(III) will be more easily to absorbed and fixed. Moreover, its start monomer, the citric acid, is inexpensive and easy to get. All of these practical values guarantee that HBP-1*x* should be an ideal material to use as a masking agent or tanning auxiliary in chrome tanning to improve chromium absorption.

CONCLUSIONS

Carboxyl-terminated hyperbranched oligomers (HBP-1*x*) with different X_n values were synthesized from citric acid through a simple operating process. HBP-1*x* retained citric acid's coordinating capability and coordinated with Cr(III) by means of chelation to give a more stable complex. Meanwhile, its introduction into the Cr(III) coordinated complex also effectively improved its stability against alkali and oxidation. Surely, HBP-1*x* is an ideal material to act as a masking agent or tanning auxiliary in chrome tanning to improve chromium absorption.

ACKNOWLEDGMENTS

This project was supported by the Light of West Scholar Development Program of the Chinese Academy of Sciences.

REFERENCES

1. Sundar, V.; Raghava, R. J.; Muralidharan, C. *J. Clean Prod.* **2002**, *10*, 69.
2. Morera, J. M.; Bartolí, E.; Chico, R.; Solé, C.; Cabeza, L. F. *J. Clean Prod.* **2011**, *19*, 2128.
3. Gutterres, M.; Aquim, P. M.; Passos, J. B.; Trierweiler, J. O. *J. Clean Prod.* **2010**, *18*, 1545.
4. Hu, J.; Xiao, Z.; Zhou, R.; Deng, W.; Wang, M.; Ma, S. *J. Clean Prod.* **2011**, *19*, 221.
5. Jian, S.; Wenyi, T.; Wuyong, C. *J. Clean Prod.* **2011**, *19*, 325.
6. Li, S.; Li, J.; Yi, J.; Shan, Z. *J. Clean Prod.* **2010**, *18*, 471.
7. Chenying, L.; Hualin, C.; Ron, L.; Bailing, L.; Minghua, L. *China Leather* **2012**, *41*, 48.
8. Grigoras, M.; Stafie, L. *High. Perform. Polym.* **2009**, *29*, 304.
9. Amin, A.; Darweesh, H. M.; Morsi, S. M. M.; Ayoub, M. M. H. *J. Appl. Polym. Sci.* **2011**, *24*, 1483.
10. Mahapatra, S. S.; Karak, N. *J. Macromol. Sci. A* **2009**, *46*, 296.
11. Petkov, V.; Parvanov, V.; Tomalia, D.; Swanson, D.; Bergstrom, D.; Vogt, T. *Solid State Commun.* **2005**, *134*, 671.
12. Wang, W.; Zheng, Y.; Roberts, E.; Christopher, J.; Ding, L.; Irvine, D. *J. Macromolecules* **2007**, *40*, 7184.
13. Amin, A.; Darweesh, H. H. M.; Ramadan, A. M.; Morsi, S. M. M.; Ayoub, M. M. H. *J. Appl. Polym. Sci.* **2011**, *121*, 309.
14. Haroun, A. A.; Masoud, R. A.; Bronco, S. *Macromol. Symp.* **2006**, *235*, 187.
15. Huimin, T.; Yunjun, L. In Hyperbranched Polymer; Shanglin, D., Ed.; Chemical Industry: Beijing, **2002**; Chapter *1*, p 16.
16. Yunjun, L.; Min, X.; Xingyuan, W. In Hyperbranched Polyester; Shanglin, D., Xuehua, X., Eds.; Chemical Industry: Beijing, **2009**; Chapter *5*, p 196.
17. Hualin, C.; Bailing, L.; Rong, L. *China Leather* **2007**, *15*, 13.
18. Xuechuan, W.; Xuzheng, Y.; Taotao, Q.; Longfang, R. *J. Soc. Leather Technol. Chem.* **2009**, *93*, 61.
19. Qiang, X.; Liu, A.; Guan, J.; Li, L.; Ma, C.; Shen, L.; Hong, X. *Fine Chem.* **2008**, *9*, 10.
20. Jing, Y.; Liqiang, L.; Yanchun, L. *China Leather* **2009**, *38*, 42.
21. Xianbo, L.; Xuechuan, W.; Taotao, Q.; Dan, Z. *China Leather* **2010**, *39*, 27.
22. Xiaoming, F.; Rongguo, C.; Liren, X.; Qinghua, C. *Polym. Int.* **2011**, *60*, 136.
23. Hualin, C.; Bailing, L.; Rong, L. *China Leather* **2006**, *35*, 18.
24. Xuechuan, W.; Yanxin, H.; Shujie, Z.; Sha, Z. *New Chem. Mater.* **2011**, *39*, 26.
25. Voit, B. I. C. R. *Chim.* **2003**, *6*, 821.
26. Namazi, H.; Adeli, M. *Biomaterials* **2005**, *26*, 1175.
27. Namazi, H.; Motamedi, S.; Namvari, M. *BioImpacts* **2011**, *1*, 63.
28. Namzai, H.; Fard, A. M. P. *Mater. Chem. Phys.* **2011**, *129*, 189.
29. Namazi, H.; Adeli, M. *Eur. Polym. J.* **2003**, *26*, 1491.
30. Akbari, S.; Kish, M. H.; Entezami, A. A. *Polym. Int.* **2008**, *57*, 846.
31. Huilin, T.; Lihong, F. *Leather Sci. Eng.* **2010**, *20*, 23.
32. Huilin, T.; Lihong, F. *Leather Chem.* **2011**, *28*, 12.
33. Zuren, P.; Jingwu, S. In Polymer Chemistry; Jing, Y., Xuehua, X., Eds.; Chemical Industry: Beijing, **2010**; Chapter *2*, p 23.
34. Tomalia, D. A.; Naylor, A. M.; Goddard, W. A., III. *Angew. Chem. Int. Ed.* **1990**, *29*, 138.
35. Huimin, T.; Yunjun, L. In Hyperbranched Polymer; Shanglin, D., Ed.; Chemical Industry: Beijing, **2002**; Chapter *2*, p 30.
36. Hölter, D.; Burgath, A.; Frey, H. *Acta Polym.* **1997**, *48*, 30.
37. Stark, B.; Stühn, B.; Frey, H.; Lach, C.; Lorenz, K.; Frick, B. *Macromolecules* **1998**, *31*, 5415.
38. Frey, H.; Holter, D. *Polym. Mater.* **1997**, *77*, 226.
39. Yongwu, C.; Guoying, L. In Tanning Chemstry; Jianhua, L., Ed.; China Light Industry: Beijing, **2008**; Chapter *2*, p 21.
40. Yongwu, C.; Guoying, L. In Tanning Chemstry; Jianhua, L., Ed.; China Light Industry: Beijing, **2008**; Chapter *2*, p 47.
41. Hongbing, Z.; Jimin, Z. *China Leather* **2004**, *33*, 51.
42. Nan, W.; Xiaoying, X.; Kunyu, W. W. *Leather* **2011**, *33*, 40.
43. Quanjie, W. *China Leather* **2012**, *41*, 39.